We would like to thank the reviewer for the effort in helping us improve the manuscript. Below we respond point-by-point to the comments.

Reviewer #1

General comments:

This study proposes a new classification of liquid water clouds based on cloud-top height and cloud-base height, the former and latter being employed to quantify cloud heterogeneity and cloud altitude, respectively. The authors employ their newly developed retrieval for cloud-base height at cloud scale. The total six cloud categories are defined as a result from three cloud-base height intervals and two intervals of cloud-top horizontal variability. It is then shown that the climatology of their occurrence is reasonable on the global scale, and two basic cloud properties (liquid water path and cloud droplet number concentration) are also documented to show some interesting differences between the categories defined. I think that the authors' analysis is a meaningful addition to current knowledge of satellite-based analysis of cloud regimes, particularly given that this study's approach of classification is based on cloud geometrical information and thus independent of cloud microphysical/optical properties. This will enable more meaningful investigation of cloud microphysical/optical properties for different cloud regimes as a function of environmental factors such as aerosol and stability conditions. I only have a couple of minor comments described below in an attempt to make the authors' analysis more sounding before the paper will be published in Atmos. Chem. Phys.

We thank the reviewer for this thoughtful and constructive statement.

Specific comments:

Overall: It would be beneficial to readers if quantitative information about retrieval uncertainty of cloud-base height and cloud-top height is provided so that readers can evaluate how robust the statistics shown in the manuscript (e.g. RFOs of different categories and PDFs of cloud properties) are.

This is a very good point and a very useful addition. Cloud base height was examined in detail by Mülmenstädt et al. (ESSD 2018), and we added a statement to the description of the data.

Line 165-170, Figure 4 and Table 1: The authors argue here that characteristics of Nd and L (in both PDFs and mean/median values) for six cloud categories show some signatures of different cloud behaviors between over continent and ocean. I would recommend the authors to separate the analysis into continent and ocean to more clearly see land-ocean differences in Nd and L in each category, facilitating the authors' interpretation and also eliminating the effect of background aerosol differences between land and ocean on cloud characteristics.

We thank the reviewer for this very useful suggestion, and now show and discuss the characteristics separately for land and ocean in an Appendix, in conjunction with the discussion of Tropics vs. extratropics as suggested by reviewer #2.

Technical comments:

Figure 1 right panel: The color bar appears to show relative scale of variability, but the text (Line 114) states that "Cloud top height variability is defined here as the average absolute deviation". Can you clarify?

We thank the reviewer for this attentive reading of the text. Indeed, it is the relative *deviation.*

Figure 2: Please add labels for horizontal axes, i.e. "cloud base height [m]" for left panel and "cloud-top height variability [%]" for right panel. It would also be helpful for readers if characters such as

“low”, “middle” and “high” are added to the corresponding ranges of cloud-base height on left panel and those such as “stratiform” and “cumuliform” are added to the corresponding range of cloud-top height variability on right panel.
The figure is revised as suggested.

Line 153: “their response to perturbations”: “perturbations” of what?
We thought specifically of aerosols and add this here.

Reviewer #2

\textit{We would like to thank the reviewer for the effort in helping us improve the manuscript. Below we respond point-by-point to the comments.}\\\par

The paper describes the use of CloudSat and CALIPSO retrievals of cloud base and cloud top heights to classify low (water) clouds in the atmosphere across the globe. The data are then combined with MODIS retrievals of number concentration and liquid water path to show the utility of the classification in distinguishing between different cloud states. The study is nice addition to the body of work on cloud classification from satellite observations. The paper is well-written and follows a logical flow of arguments. Its weaknesses lie in an incomplete description of the techniques applied as well as a lack of discussion of some obvious caveats in the results. I expand on both in my comments below. These issues should be straightforward to address and the paper will be acceptable for publication once they are.\\
\textit{*We thank the reviewer for the careful evaluation of the manuscript.*}\\\par

Major comments\\
Description of the techniques used:\\
Lines 62-65: The paragraph introduces the CCCM data set that forms the foundation of this study. For the reader to fully comprehend how the classification works and how it might later link to the MODIS retrievals it is necessary to add a short paragraph here that provides a little more detail on how this merged product was created. How is the vertically resolved but horizontally sparse CloudSat and CALIPSO data combined with horizontally resolved MODIS data? What does it mean to use the CloudSat and CALIPSO data on a 20 km footprint? I realise there is a set of papers to read up on this, but not only would it help attract a greater readership if a short summary was provided here, it is also essential to understand the results that follow.\\
\textit{*The reviewer is right that it is better to add a short statement about how the colleagues at NASA Langley did the work to create the CCCM dataset, rather than just referencing their papers. We added a paragraph explaining the details of the procedure.*}\\\par

Line 117: You mention the use of adjacent footprints to look at the variability. What does adjacent mean here? Adjacent in which direction? I assume it is adjacent along the Aqua track? Please provide a little more detail here. \\
\textit{*The reviewer is correct with her/his assumption, and we now clarify this in the revised manuscript.*}\\\par

Discussion of caveats\\

The biggest caveat of the study is that the choice of looking at liquid water clouds only automatically introduces a geographic distribution to the result. This is so, because the 0C level in the tropics is at 5 (or so) km and in the polar regions it's very low (or even non-existent). This will bias liquid water path to be larger in the tropics and smaller in the extratropics. As the cloud classes show a strong geographic distribution (Figure 3), the separation of liquid water path by cloud class in Figure 4 could simply be a geographic sampling issue and have nothing to do with cloud-aerosol interactions. There is probably little you can really do about this at the definition stage, but you can account for it in the analysis of N_d and L and you MUST discuss that this as an issue in your conclusions.\\
\textit{*The reviewer is right that this is an important caveat and we clearly now state it in the conclusions.* }\\\par

I recommend to reduce this issue by performing analyses of the N_d and L pdfs in selected regions. As a minimum one might want to separate the (warm) tropics from the (cold) extra tropics. You could then contrast say land and ocean in both regions and see if something useful emerges. That way you can alleviate at least some of the concern that the L differences are just difference in physical thickness resulting from the fact that different cloud classes preferably occur in the tropics (e.g., inhomogeneous C_B,mid) or the mid-latitudes (C_B,low). \\
Places where this fits in the manuscript are near line 165 or 175 and in the summary and conclusions.
\textit{*This is a very sensible suggestion. We now analyse and discuss separately Tropics and extratropics in a new Appendix, in conjunction with the discussion of oceanic vs. continental clouds as suggested by reviewer #1.*}\\\par

Minor comments (on chronological order)
Line 29: Parentheses missing around the citations.
\textit{*Corrected, thanks!*}\\\par

Line 96: Why do you use "roughly terciles" rather than terciles? How rough is rough? What are the tercile values compared to what you use? Presumably you just want round numbers or is there more to it?\\
\textit{*Indeed, this was just to use round numbers. We clarify it in the text.*}\\\par

Line 101: Add 'and' between homogeneous and cumuliform\\
\textit{*This indeed needs better style. We chose to put a comma instead of an "and".*}\\\par

Line 121: Actually, the shallow Cu regions show remarkably little variance compared to the deep tropics! As you are only using water clouds and therefore exclude deep convection, this is a little surprising. Is this a physical signal or is there something difficult about your method in the deep tropics that might cause this result? Please discuss this more deeply.\\
\textit{*Over the Pacific and Indian oceans, the variability in the shallow cu regions, in fact, is rather elevated; it is lower than in the Tropics mostly in the southern Atlantic ocean that we chose to center our figure on. We added a discussion, as recommended by the reviewer.*}\\\par

Line 124: The statement that your classification can separate stratiform and cumuliform is true to first order, but the trade regime, which is mostly cumuliform, does not show up very strongly. This makes sense as the inversions there are still quite strong and even though the clouds might be cumuliform, their tops are tightly constrained by the inversion height. So there is a caveat on your simple inhomogeneity assumption here, that you should acknowledge.\\
\textit{*The reviewer is right, and we write a statement on this now in the revised manuscript.*}\\\par

Line 130: Delete: ‘Consistent with the expectation’, as this certainly was not my expectation and might not be that of all readers.\\
\textit{*Done as suggested.*}\\\par

Figure 3: Bottom right panel is mislabeled.\\
\textit{*The figure is revised as suggested.*}\\\par

Line 136: The low H-base clouds nicely follow regions of low SST. It might be worth mentioning this here.\\
\textit{*Thanks for this, we do this in the revised manuscript.*}\\\par

Line 139 and through the paper: I believe it is dangerous to refer to you classes as “mid-level clouds” or “high clouds”, as they are not. Please be diligent in using terms like low-base, mid-level-base or high-base clouds. You do this in parts already and it is important to stick to that to minimise confusion with real mid-level or high clouds in the atmosphere. Please go carefully through the entire manuscript to fix this everywhere. \\
\textit{*The reviewer is right, and we follow this advice.*}\\\par

Summary and conclusions section: Please add a short discussion as what you perceive to be the weaknesses of your methodology and how those could be addressed in future work.\\
\textit{*We take up the earlier comment by the reviewer and note this could be enhanced to characterize all clouds, not just the liquid ones. We also describe how the study might be enhanced by using passive retrievals of cloud-base height via triangulation from e.g. MISR.*}

A new classification of satellite derived liquid water cloud regimes at cloud scale

Claudia Unglaub[1], Karoline Block[1], Johannes Mülmenstädt[1,2], Odran Sourdeval[1,3], and Johannes Quaas[1]

[1]Universität Leipzig, Institute for Meteorology, Stephanstr. 3, 04103 Leipzig

[2]now at Pacific Northwest National Laboratory, Richland

[3]now at Laboratoire d'Opique Atmosphérique, Université de Lille

Correspondence: Johannes Quaas (johannes.quaas@uni-leipzig.de)

Abstract. Clouds are highly variable in time and space affecting climate sensitivity and climate change. To study and distinguish the different influences of clouds on the climate system it is useful to separate clouds into individual cloud regimes. In this work we present a new cloud classification for liquid water clouds at cloud scale defined using cloud parameters retrieved from combined satellite measurements from CloudSat and CALIPSO. The idea is that cloud heterogeneity is a measure that allows to distinguish cumuliform and stratiform clouds, and cloud base height a measure to distinguish cloud altitude. The approach makes use of a newly-developed cloud-base height retrieval. Using three cloud base height intervals and two intervals of cloud top variability as an inhomogeneity parameter provides six new liquid cloud classes. The results show a smooth transition between marine and continental clouds as well as between stratiform and cumuliform clouds in different latitudes at the high spatial resolution of about $20\,\mathrm{km}$. Analyzing the micro- and macrophysical cloud parameters from collocated combined MODIS, CloudSat and CALIPSO retrievals shows distinct characteristics for each cloud regimes that are in agreement with expectation and literature. This demonstrates the usefulness of the classification.

1 Introduction

Clouds affect the climate system in a wide varieties of ways. They influence outgoing solar and terrestrial radiation and therefore the Earth's temperature, produce precipitation, transport heat and moisture and interact with the surrounding atmosphere including aerosols on different time and spatial scales. They exhibit a high variability from minutes to days in time and meters to thousands of kilometer in space. Because of their complexity, the response of clouds to perturbations remains one of the largest uncertainties in climate prediction (e. g., Boucher et al., 2013). Different cloud regimes have different impacts on climate. Low clouds and optical thick clouds contribute to cooling the climate system because their high albedo effect dominates their effect on emitted longwave radiation back to space (Hartmann et al., 1992) whereas thin medium and high altitude clouds rather contribute to warming the climate system (Dhuria and Kyle, 1990).

Consequently, since the early start of meteorological research, clouds have been classified (Howard, 1803). A fundamental distinction usually is made by cloud altitude (often in three classes of low, middle and high tropospheric clouds, WMO, 1975) as well as the separation of stratiform and cumuliform clouds (WMO, 1975, 2017).

Cloud types are often defined using the dynamical state of the atmosphere, or, alternatively, using cloud parameters themselves, or a mix of both. Dynamical regimes are often based on large scale, mid-tropospheric vertical velocity ($\omega_{500\,\mathrm{hPa}}$) derived from meteorological model reanalysis (e. g., Bony et al., 2004; Norris and Weaver, 2001). Also the lower-tropospheric stability (LTS; Klein and Hartmann, 1993) or, alternatively, the estimated inversion strength (EIS; Wood and Bretherton, 2006) or estimated low-level cloud fraction ~~Park and Shin (2019); Shin and Park (2019)~~ (Park and Shin, 2019; Shin and Park, 2019) have been used to characterise low-level clouds; some studies have used a combination of mid-tropospheric vertical velocity and LTS/EIS (Su et al., 2010; Medeiros and Stevens, 2011). Tselioudis et al. (2000) use the sea level pressure to define three different dynamical cloud types in the northern midlatitudes, and Ringer and Allan (2004) combine sea surface temperature and $\omega_{500\,\mathrm{hPa}}$. As a prime example of the other method, the International Satellite Cloud Climatology Project (ISCCP) cloud classification uses cloud optical thickness, τ_c, and cloud top pressure p_top to separate 49 or, in a simplified version, nine cloud types (Rossow and Schiffer, 1999). By applying a clustering algorithm to these ISCCP cloud classes, Jakob et al. (2005) defined four cloud regimes in the tropical western Pacific using τ_c, p_top and the total cloud cover f_tot. Extending and simplifying this approach for climate model evaluation, Williams and Webb (2008) selected different cloud regimes in particular geographical regions using cloud albedo, p_top and total cloud cover, f_tot. Such a regime definition was also found useful in the context of the analysis of aerosol optical depth-cloud droplet concentration using satellite data in the study of Gryspeerdt and Stier (2012).

We are interested to statistically analyse aerosol-cloud interactions in satellite data beyond the aerosol-droplet concentration relationship. In order to identify aerosol-cloud interactions, Stevens and Feingold (2009) suggested that it is necessary to do so for individual cloud regimes ~~(Mülmenstädt and Feingold, 2018, see also)~~(see also Mülmenstädt and Feingold, 2018). However, a dynamical regime definition is hampered by the problem of a rather coarse resolution of the reanalysis data (50-100 km currently) and the problem that thus such cloud regimes are not able to separate clouds at the scale of individual cloud regimes ~~Nam and Quaas (2013)~~(Nam and Quaas, 2013). In turn, the approach to use the ISCCP cloud definition (e.g., Jakob et al., 2005) is not useful to analyse aerosol-cloud interactions if one is interested in analysing how cloud fraction and cloud albedo co-vary with the aerosol since these quantities are fixed by the clustering method.

In this work we present a new cloud classification at cloud scale using the cloud base height indicating meteorological conditions and separating cloud altitude, and the cloud top variability as an inhomogeneity parameter separating between stratiform and cumuliform clouds. The collocated satellite data and the high spatial resolution defined as the Clouds and the Earth's Radiant Energy System (CERES) ~~Footprint~~ footprint size of about 20 km allow a cloud class based analysis of cloud parameter reflecting the high spatial and temporal variability.

2 Satellite data

Our studies rely on retrievals of two active satellite instruments, the Cloud Profiling Radar ~~(CPR, Stephens et al., 2008; Haynes et al., 2009)~~ (CPR; Stephens et al., 2008; Haynes et al., 2009) onboard CloudSat and the Cloud-Aerosol LIdar with Orthogonal Polarization ~~(CALIOP, Winker et al., 2007, 2009)~~ (CALIOP; Winker et al., 2007, 2009) onboard Cloud-Aerosol Lidar and Infrared Pathfinder Satellite Observations (CALIPSO), as well as the passive ~~Moderating~~ Moderate Resolution Imaging Spectroradiometer ~~(MODIS Barnes et a~~

(MODIS; Barnes et al., 1998; King et al., 2003; Platnick et al., 2003) instrument onboard Aqua. These satellites are part of the A-Train satellite constellation (Stephens et al., 2002, 2018), a group of satellites flying along nearly the same polar orbital track crossing the equator at about 13:30 local time and providing a global data coverage between 82°N and 82°S (Winker et al., 2007; Tanelli et al., 2008). The sun-synchronous polar orbit repeats the same ground track every 16 days retaining its size and shape (Stephens et al., 2008).

The CALIPSO CloudSat CERES and MODIS merged product (CCCM dataset) contains collocated data from CALIOP, CPR, MODIS and the broadband radiometer CERES providing comprehensive informations about clouds, aerosols and radiation fluxes in high vertical and horizontal resolution (Kato et al., 2010, 2011), merged to the CERES footprint of about 20 km horizontal size. It is this combined product that is the basis for our analysis. The collocation of these various retrievals with different spatial resolution requires a two step process. In the first step the vertical cloud profiles as provided in the Vertical feature mask from CALIPSO (Winker et al., 2007) and the 2B-Cldclass product from CloudSat (Stephens et al., 2008) are collocated on a horizontal 1 km × 1 km grid. Each grid point contains three vertical cloud profiles from CALIPLSO, and one from CloudSat, these are used to derive cloud top heights and cloud base heights (Kato et al., 2010). With this merging procedure about 85% of the cloud top heights and 77% of the cloud base heights are derived from CALIPSO measurements. The second step starts with collocating horizontally the merged vertical cloud profiles with CERES footprints of about 20 km size by selecting the CERES footprints with maximum overlap with the CALIPSO-CloudSat ground track. Because the horizontal resolution of CERES is much coarser than the horizontal resolution of the combined CloudSat/CALIPSO vertical cloud profiles, at each grid box, CloudSat/CALIPSO clouds groups are defined to retain the statistical cloud geometric information.

The temperature profiles included in the CCCM dataset are derived at computational levels from the CERES Meteorological, Ozone, and Aerosol (MOA) analysis. They come from the Global Modeling and Assimilation Office (GMAO) Goddard Earth Observing System (GEOS)-4 (Bloom et al., 2005) Data Assimilation System reanalysis before November 2007 and GEOS-5 (Rienecker et al., 2008) thereafter (Kato et al., 2014) with a temporal resolution of 6 h and a spatial resolution of $1^\circ \times 1^\circ$ (Kato et al., 2011).

A key parameter used in this paper is cloud base height, H_{base}. This relies on a new retrieval on the basis of CALIPSO lidar described by Mülmenstädt et al. (2018) that assumes that H_{base} is constant in a scene, and that the lowest lidar return within columns that do not fully attenuate the lidar beam is representative for H_{base}. Besides H_{base}, also cloud top height, H_{top}, is used as derived from the CALIPSO in the merged vertical cloud profiles. Mülmenstädt et al. (2018) thoroughly examined the cloud-base altitude using ground-based ceilometer data as reference. The root-mean-square-error on retrieved cloud base height was in the range of 400 to 700 m, and biases much lower at 5 to 50 m. Both parameters are defined here with respect to the surface altitude.

Cloud top temperature T_{top} is taken from MODIS and CloudSat/CALIPSO as derived from their respective H_{top} assigned to T_{top} using the temperature profile. Further, cloud optical thickness, τ_{c}, and, cloud droplet effective radius, r_{eff}, as derived from MODIS measurements are analysed. We use retrievals that apply the 3.7 μm channel (Platnick, 2002; Platnick et al., 2003; Painemal and Zuidema, 2011).

Daytime data are used, and high latitudes (polewards of 60°) are excluded to avoid biases in the retrieved cloud optical prop-

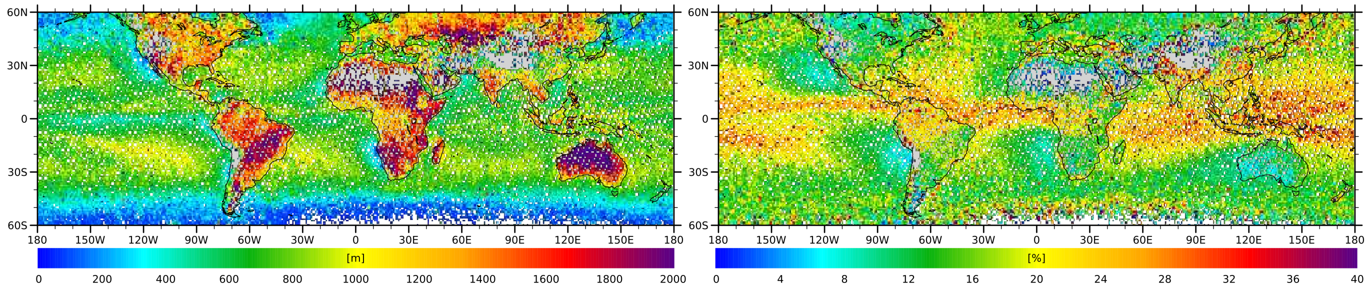

Figure 1. Time-average distributions of daily values for the 2007 - 2010 period of CALIPSO retrievals as reported in the CCCM dataset for liquid-water clouds for (a) cloud-base altitude (using the retrieval method of Mülmenstädt et al., 2018), and (b) cloud top height variability.

erties from MODIS (Zeng et al., 2012; Grosvenor et al., 2018). Our studies investigate only liquid water clouds. These are defined as clouds where T_{top} derived from both MODIS and CloudSat/CALIPSO are larger than $273\,\mathrm{K}$.

3 Definition of the cloud classes

The liquid cloud classes are defined at the scale of the CERES footprint size of about $20\,\mathrm{km}$ as horizontal resolution, at which the CCCM dataset is generated. This results in one liquid cloud type per footprint after the cloud classification process described in the following.

3.1 Cloud base height

The first cloud parameter selected to define the cloud classes is cloud base height over ground H_{base}. This is consistent with the WMO definition of cloud altitude (WMO, 1975, 2017). H_{base} is used from the retrieval approach of Mülmenstädt et al. (2018), applied to the CCCM dataset. H_{base} of a multilayer clouds is defined as the lowest H_{base} in this cloud group. In Fig. 1 the global distribution of the averaged H_{base} of the four completely available years of CCCM data from 2007 to 2010 is shown. One can see a clear contrast between land and ocean and between higher and lower latitudes. The lowest H_{base} are located over the ocean in the storm track regions in mid latitudes whereas the highest H_{base} can be found over land for example over the Amazon rain forest or Australia.

To separate different cloud base height classes the probability density function (PDF) of the global spatiotemporal distribution of H_{base} shown in Fig. 2 is used. Three cloud base height classes are selected which are ~~roughly~~ the round numbers that approximately correspond to the terciles of the distribution~~and are defined as~~, which is the median $\pm 300\,\mathrm{m}$. With this definition, *low* clouds are defined as those with $H_{\mathrm{base}} \leq 350\,\mathrm{m}$; *middle* clouds for $350\,\mathrm{m} < H_{\mathrm{base}} \leq 950\,\mathrm{m}$; and *high* (liquid) clouds for $H_{\mathrm{base}} > 950\,\mathrm{m}$.

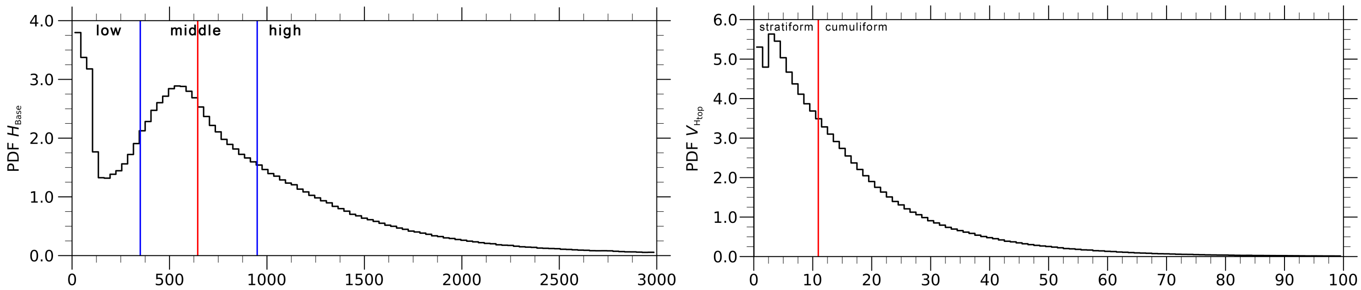

Figure 2. PDFs of the spatiotemporal distributions of (a) of cloud base height (m) and (b) cloud-top height variability (%), for daily data for the four-year period 2007 to 2010. The red lines indicate the median of the PDFs and the two blue lines in (a) represent the borders of the cloud base classes.

3.2 Cloud top variability as inhomogeneity parameter

Only using H_{base} one cannot distinguish between cumuliform and stratiform clouds as proposed by the WMO. We propose to use an inhomogeneity parameter and define stratiform clouds as homogeneous, cumuliform clouds as inhomogeneous clouds. Cloud optical thickness, τ_{c}, is often used to describe the inhomogeneity of a cloud or cloud field and to separate clouds into homogeneous and inhomogeneous clouds. The ISCCP cloud classification uses τ_{c} itself to classify stratiform and cumuliform clouds, defining clouds with high τ_{c} as stratiform (Rossow and Schiffer, 1999). In a more advanced approach, the horizontal variablity of τ_{c} derived from MODIS measurements is defined as cloud inhomogeneity parameter to distinguish stratiform and cumuliform clouds (Oreopoulos and Cahalan, 2005).

With the definition proposed here for cloud regimes, however, we aim to analyse adjustments to aersol-cloud interactions (e.g., Mülmenstädt and Feingold, 2018), i.e. the response of cloud liquid water path to perturbations in cloud droplet concentrations (e.g., Gryspeerdt et al., 2019). It is thus impossible to use τ_{c} to define cloud regimes, since this would constrain liquid water path.

We thus propose to define cloud inhomogeneity based on the cloud top height variability. Cloud top height is related to τ_{c} and also H_{base}, but its variability is independent of it. The idea is that clouds with horizontally homogeneous top heights are more stratiform, and those with horizontally inhomogeneous top heights more cumuliform. Cloud top height variability is defined here as the average ~~absolute~~ relative deviation of cloud top heights from its footprint mean. Preliminary analysis of the cloud-top height variability at the scale of a CERES footprint, given the MODIS resolution, often is not well defined, at least in broken-cloud situations. This is due to the too low number of MODIS retrievals within a CERES footprint. Thus, the variability in the two adjacent footprints (adjacent along the A-Train ground track), in addition to the footprint at nadir below the satellite is used, and the average cloud-top height variability weighted by cloud occurrence in the three footprints, is used.

In Fig. 1, the global distribution of the mean cloud top variability from 2007 to 2010 is shown. No clear land-ocean contrast is seen, but the distribution is characterized by a latitudinal gradient with the highest values of cloud top variability in the tropics in the shallow cumulus regions and along the Intertropical Convergence Zone (ITCZ). In the shallow cumulus regions

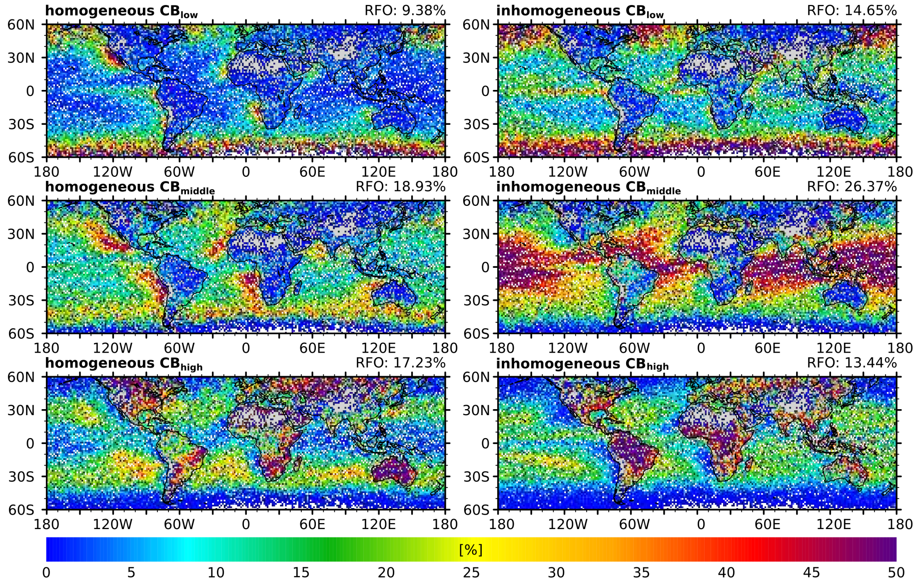

Figure 3. Relative frequency of occurrence of the six cloud classes separated using the three classes of cloud-base height and two classes of cloud-top height heterogeneity. Top row - low, middle - mid, bottom - high clouds; left column - homogeneous (stratiform), right column - heterogeneous (cumulisform) clouds.

towards the western parts of the oceans in the sub-tropics, the variability is – with values between 20 and 30% – about as large as in the Tropics for the Indian and Pacific oceans, it is, however, somewhat lower in particular in the southern Atlantic ocean. At mid- to high latitudes the mean cloud top variability decreases in general, compared to the tropical regions. Although at low latitudes, the stratocumulus decks west South Africa, South America and North America show the smallest mean cloud top variabilities. These features are consistent with the hypothesis that the heterogeneity metric is useful to distinguish stratiform and cumuliform clouds. However, it is not a perfect classification into stratiform and cumuliform clouds e.g. for suppressed shallow convection where the cloud top altitude is dictated by subsidence. The PDF of the cloud top variability shown in Fig. 2 is used to make this distinction. The median at about 11% separates the more stratiform (homogeneous) clouds from more cumuliform (inhomogeneous) clouds creating two inhomogeneity cloud classes.

3.3 Geographical distribution of the cloud regimes

The three cloud base classes and two inhomogeneity cloud classes are now combined to define six new liquid water cloud types or cloud regimes. The global distribution of relative frequencies of occurence (RFOs) of these cloud classes is shown in Fig. 3. ~~Consistent with the expectation, clouds with~~ Clouds with low and mid base altitude tend to be more heterogeneous, and clouds with high base altitude, more homogeneous. Low and mid clouds tend to occcur over ocean rather than land, although the contrast is less strong for stratiform clouds.

Most of the liquid water clouds with low H_{base} are located over the ocean in the storm track regions in mid to high latitudes. Only a small amount of the low clouds occur in low latitudes. Homogeneous low clouds concentrate in mid latitudes especially in the Southern hemisphere and in narrow coastal stripes west of North and South America and North and South Africa indicating parts of the typical stratocumulus clouds in these regions with very low H_{base}. The occurrence is highest over regions with relatively low sea surface temperatures. The inhomogeneous clouds in this cloud base class occur mainly in the mid latitudes in both hemispheres though a small amount can be found in tropical regions especially along the ITCZ in the east Pacific.

Almost all mid-level mid-level-base clouds are marine clouds located over the oceans in low latitudes. Especially in the tropics along the ITCZ in the Indian ocean and in the west Pacific this cloud class is frequent. Inhomogeneous clouds in this cloud base class extend in low latitudes around the entire globe leaving out the stratocumulus decks and concentrate mainly in shallow cumulus regions and along the ITCZ.

In contrast to the cloud base classes of lower H_{base} most of the high clouds occur over land. However, a non-negligible amount can be found over the ocean in low latitudes. Only in higher latitudes over the ocean and in the stratocumulus regions in the east Pacific and east Atlantic almost no clouds with $H_{\mathrm{base}} > 950\,\mathrm{m}$ are found. A significant amount of homogeneous clouds in this cloud base class are located over land with maxima over South Africa, Australia and north west Asia. Over the ocean they cover two bands in both hemispheres at around 30° leaving out roughly the areas covered by the inhomogeneous mid-level mid-level-base clouds. The inhomogeneous high-level high-base clouds occur mainly over land with maxima over rain forest regions in South America and middle Africa. Over ocean these clouds can be found equally distributed to inhomogeneous clouds in low latitudes except in the stratocumulus decks.

4 Cloud properties in the six cloud regimes

The key reason to define cloud regimes is that clouds are supposed to show different characteristics in these regimes. The hypothesis is that their response to perturbations e.g. of aerosol concentrations possibly can be identified more clearly in analyses when focusing on individual regimes (Mülmenstädt and Feingold, 2018). The goal of this section is to demonstrate the usefulness of the separation in cloud regimes according to the six classes defined in the previous section. To this end, the two main bulk cloud quantities are investigated, namely the cloud liquid water path, L, and the cloud droplet number concentration, N_{d}. Both are computed on the basis of the MODIS bi-spectral retrievals as reported in the CCCM dataset. N_{d} is computed from the retrieved cloud optical thickness and cloud-top droplet effective radius following Grosvenor et al. (2018) and the parameters defined in Quaas et al. (2006).

Cloud droplet number concentration is a key quantity when assessing aerosol-cloud interactions and cloud radiative effects (e.g., Grosvenor et al., 2018). It depends on chemical composition and size distribution of the precursor aerosol, as well as cloud-base vertical velocity (Barahona et al., 2011). It is also very much influenced by cloud- and precipitation microphysical processes (Wood et al., 2012) as well as cloud-top and cloud-side entrainment.

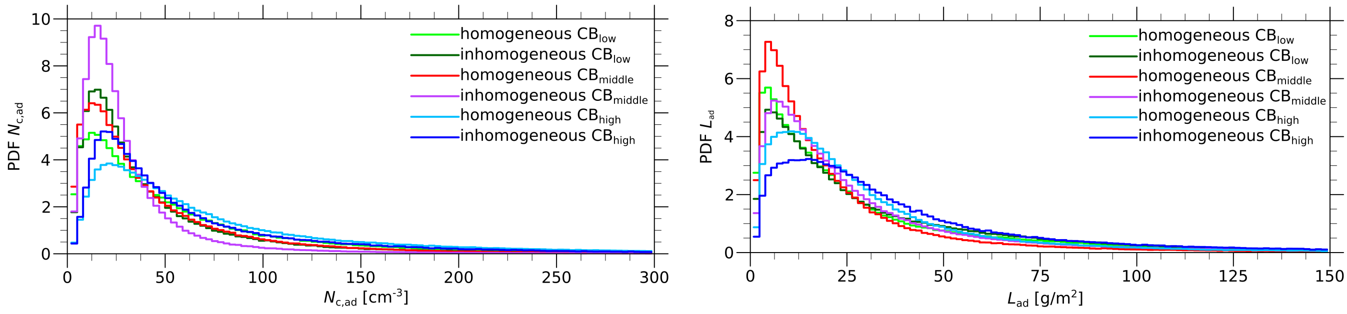

Figure 4. PDFs of the spatio-temporal distribution of four years (2007 – 2010) of MODIS retrievals as reported in the CCCM dataset at the $20\times20\,\mathrm{km}^2$ horizontal resolution at nadir below the A-Train satellite constellation, between 60°S and 60°N. Liquid clouds are selected. Light green - low, homogeneous clouds; dark green - low, heterogeneous clouds; red - middle, homogeneous clouds; purple - middle, heterogeneous clouds; light blue - high, homogeneous clouds; dark blue - high, heteorgeneous clouds. (a) for droplet number concentration, N_d (cm^{-3}), (b) liquid water path, L (g m^{-2}).

Cloud Classes	Low		Middle		High	
	N_d	L	N_d	L	N_d	L
Homogeneous, mean	76 cm^{-3}	33 g m^{-2}	49 cm^{-3}	24 g m^{-2}	91 cm^{-3}	33 g m^{-2}
median	39 cm^{-3}	19 g m^{-2}	29 cm^{-3}	14 g m^{-2}	54 cm^{-3}	21 g m^{-2}
Inhomogeneous, mean	55 cm^{-3}	36 g m^{-2}	34 cm^{-3}	32 g m^{-2}	73 cm^{-3}	45 g m^{-2}
median	28 cm^{-3}	21 g m^{-2}	21 cm^{-3}	19 g m^{-2}	~~47 cm^{-3}~~ 42 cm^{-3}	28 g m^{-2}

Table 1. Average (blue) and median (red) values of N_d and L for the six particular cloud classes derived from their PDFs (Fig. 4).

Fig. 4 shows the global PDF of N_d for the six cloud regimes, and Table 1 summarizes the mean and median values. The values are clearly distinct between the six classes. One key feature is that for all cloud-base heights, the homogeneous clouds contain fewer droplets than the heterogeneous ones. This is consistent with the expectation that heterogenous, convective clouds are driven by stronger updraughts. In terms of the altitude classes, ~~low-level~~ low-base clouds show more droplets than ~~mid-level~~ mid-level-base clouds. This is a feature of the geographical distribution: both types occur mostly over oceans, but the ~~mid-level~~ mid-level-base clouds are more prevalent over the pristine parts of the oceans. The highest N_d is observed for the high clouds, due to the fact that high clouds mostly occur over continents.

Also in terms of liquid water path, L, the clouds in the six classes are distinct. Homogeneous, i.e. more stratiform clouds, are thinner than the heterogeneous counterparts in each altitude class. This is consistent with the fact that convective clouds tend to develop more in the vertical, compared to stratiform clouds. Among the cloud altitude classes, L is smallest for ~~mid-level~~ mid-level-base clouds and largest for high clouds. Note that these clouds are only the liquid-water clouds, so that the vertical development is limited by the 0°C level in our definition. Here, low clouds have the largest potential to develop in the vertical and yet remain liquid. Over land, where high cloud bases are prevalent, the 0° level is reached at higher altitudes, allowing these clouds to develop further in the vertical. Due to the choice made here to investigate only liquid water clouds, the behaviour is different in different latitudes and seasons, due to the fact that the freezing level is at lower heights in higher latitudes and winter times. More detail of the geographical variation of the cloud regimes is provided in the Appendix, where the cloud properties for the different regimes are compared for land vs. ocean, and Tropics vs. Extratropics.

5 Summary and conclusions

The goal of the present study was to overcome limitations in the definition of cloud regimes. Such a definition is desirable e.g. in the context of studying aerosol-cloud interactions. Previous approaches were either at the comparatively very coarse resolution of meteorological re-analyses or used cloud parameters that are, however, the ones to study in aerosol-cloud interaction and thus cannot be used to stratify the data. Also, previous approaches were not very compatible with the standard WMO definitions. Here, we propose six cloud regimes for liquid clouds, separated by (i) cloud-base height and (ii) cloud top-height variability as an inhomogeneity parameter. Both parameters are derived from active remote sensing satellite measurements and are thus available at the scale of satellite retrievals. They are evaluated using a four year (2007 to 2010) dataset of combined A-Train satellite data in the CCCM dataset. A new approach to retrieve cloud-base altitude from spaceborne lidar has recently been developed and applied here. The geographical distributions of the frequency of occurrence of the six cloud regimes shows desirable features: oceanic and continental clouds are smoothly separated, and typical cloud regimes such as stratocumulus decks are readily identified. In order to demonstrate the usefulness of the cloud regimes, cloud parameters not used to define the regimes, but useful to study e.g. aerosol-cloud interactions, have been analysed. The selected parameters are cloud droplet concentration and cloud liquid water path. From the analysis it is evident that the cloud regimes show different characteristics in both quantities, i.e. the cloud types are clearly distinct. In particular, expected features of homogeneous (interpreted as stratiform) and heterogeneous (interpreted as cumuliform) clouds appear, as to features related to predominant aerosol sources and boundary-layer dynamics.

In future work, the study could be enhanced to study all clouds, and not just the liquid-water ones as done in the present study. While the cloud classification method could be adapted in a straightforward way, this would require a new analysis of how the classes differ in their characteristics. The current study is limited by the fact that it can only be applied to the ground-track below the A-Train lidar and radar retrievals. However, approaches exist to infer cloud-base altitude also from passive, multi-angle measurements (Böhm et al., 2019). An adaptation of our method to these swath data would allow to analyse much larger data volumes.

Appendix A: Regime analysis by large-scale region

More detail about the characterization of N_d and L by cloud regime is provided in Figs. A1 and A2 and summarized in Table A1. The PDFs of N_d (Fig. A1) and L (Fig. A2) are separated into oceanic and continental surfaces, and between Tropics

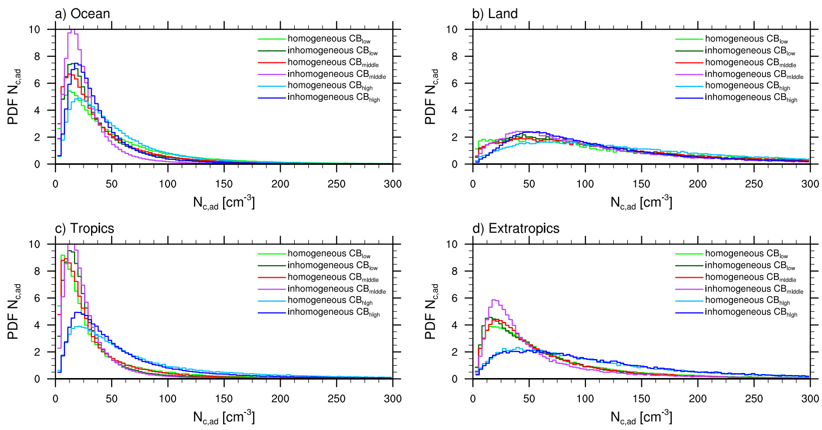

Figure A1. As Fig. 4a, but separately for (a) ocean, (b) land, (c) Tropics (20° S- 20° N) and (d) Extratropics (40° S - 60° S and 40° N - 60° N).

and Extratropics, respectively. The droplet concentrations are somewhat lower over ocean compared to the global mean, but are by factors of two to four higher over land (there are many more data points for liquid-water cloud retrievals over ocean than over land) in all cloud regimes, consistent with the expectation. The result of smaller N_d for inhomogeneous vs. homogeneous clouds holds for all categories over both, land and ocean. Liquid water path on average is slightly lower over ocean, slightly larger over land, except for the high clouds where things are rather similar. That inhomogeneous clouds have higher L holds true over both land and ocean, with the exception of the low clouds over land. Clouds in the Tropics have larger N_d than in the Extratropics, and they also have larger L (except for those with high cloud bases).

Data availability. All analyses are based on the publicly available CCCM dataset (Kato et al., 2010, 2011).

Author contributions. CU and JQ designed the research with input from all authors. OS and JM prepared the satellite data. CU and KB performed the data analysis with support by all other authors. CU and JQ wrote the manuscript with input from all authors.

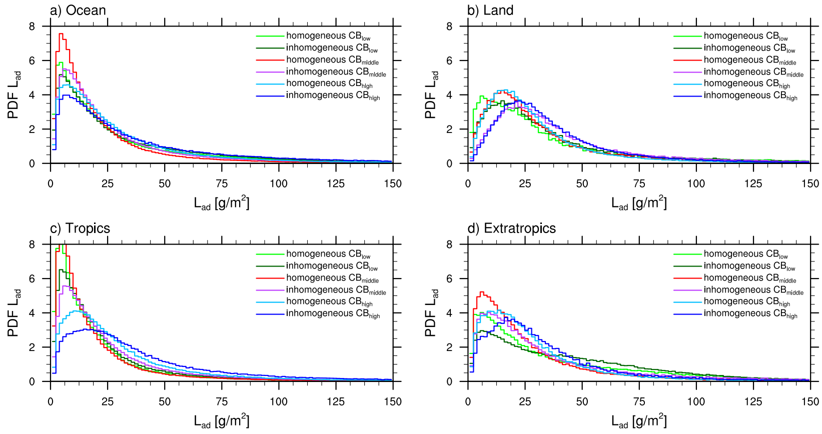

Figure A2. As Fig. 4b, but separately for (a) ocean, (b) land, (c) Tropics (20° S- 20° N) and (d) Extratropics (40° S - 60° S and 40° N - 60° N).

Competing interests. The authors declare that they have no conflict of interest.

Acknowledgements. This study was supported by the European Research Council starting grant "QUAERERE" (GA 306284). The authors are grateful to the satellite retrieval science teams for the CALIPSO, CloudSat and MODIS instruments, and in particular Seiji Kato and his coworkers at NASA Langley for compiling the CCCM dataset and helping with questions. The authors wish to thank two anonymous reviewers for their constructive comments.

	Cloud Classes	Low		Middle		High	
		N_d	L	N_d	L	N_d	L
Ocean	Homogeneous, mean	$67\,\mathrm{cm^{-3}}$	$32\,\mathrm{g\,m^{-2}}$	$43\,\mathrm{cm^{-3}}$	$23\,\mathrm{g\,m^{-2}}$	$55\,\mathrm{cm^{-3}}$	$33\,\mathrm{g\,m^{-2}}$
	median	$36\,\mathrm{cm^{-3}}$	$18\,\mathrm{g\,m^{-2}}$	$27\,\mathrm{cm^{-3}}$	$14\,\mathrm{g\,m^{-2}}$	$40\,\mathrm{cm^{-3}}$	$20\,\mathrm{g\,m^{-2}}$
	Inhomogeneous, mean	$46\,\mathrm{cm^{-3}}$	$36\,\mathrm{g\,m^{-2}}$	$28\,\mathrm{cm^{-3}}$	$31\,\mathrm{g\,m^{-2}}$	$40\,\mathrm{cm^{-3}}$	$47\,\mathrm{g\,m^{-2}}$
	median	$26\,\mathrm{cm^{-3}}$	$21\,\mathrm{g\,m^{-2}}$	$20\,\mathrm{cm^{-3}}$	$18\,\mathrm{g\,m^{-2}}$	$29\,\mathrm{cm^{-3}}$	$27\,\mathrm{g\,m^{-2}}$
Land	Homogeneous, mean	$163\,\mathrm{cm^{-3}}$	$43\,\mathrm{g\,m^{-2}}$	$141\,\mathrm{cm^{-3}}$	$37\,\mathrm{g\,m^{-2}}$	$174\,\mathrm{cm^{-3}}$	$33\,\mathrm{g\,m^{-2}}$
	median	$107\,\mathrm{cm^{-3}}$	$24\,\mathrm{g\,m^{-2}}$	$103\,\mathrm{cm^{-3}}$	$23\,\mathrm{g\,m^{-2}}$	$131\,\mathrm{cm^{-3}}$	$23\,\mathrm{g\,m^{-2}}$
	Inhomogeneous, mean	$145\,\mathrm{cm^{-3}}$	$42\,\mathrm{g\,m^{-2}}$	$121\,\mathrm{cm^{-3}}$	$47\,\mathrm{g\,m^{-2}}$	$129\,\mathrm{cm^{-3}}$	$42\,\mathrm{g\,m^{-2}}$
	median	$98\,\mathrm{cm^{-3}}$	$26\,\mathrm{g\,m^{-2}}$	$85\,\mathrm{cm^{-3}}$	$32\,\mathrm{g\,m^{-2}}$	$93\,\mathrm{cm^{-3}}$	$30\,\mathrm{g\,m^{-2}}$
Tropics	Homogeneous, mean	$42\,\mathrm{cm^{-3}}$	$22\,\mathrm{g\,m^{-2}}$	$35\,\mathrm{cm^{-3}}$	$21\,\mathrm{g\,m^{-2}}$	$87\,\mathrm{cm^{-3}}$	$34\,\mathrm{g\,m^{-2}}$
	median	$21\,\mathrm{cm^{-3}}$	$13\,\mathrm{g\,m^{-2}}$	$20\,\mathrm{cm^{-3}}$	$12\,\mathrm{g\,m^{-2}}$	$52\,\mathrm{cm^{-3}}$	$22\,\mathrm{g\,m^{-2}}$
	Inhomogeneous, mean	$33\,\mathrm{cm^{-3}}$	$27\,\mathrm{g\,m^{-2}}$	$28\,\mathrm{cm^{-3}}$	$30\,\mathrm{g\,m^{-2}}$	$66\,\mathrm{cm^{-3}}$	$47\,\mathrm{g\,m^{-2}}$
	median	$20\,\mathrm{cm^{-3}}$	$15\,\mathrm{g\,m^{-2}}$	$20\,\mathrm{cm^{-3}}$	$18\,\mathrm{g\,m^{-2}}$	$42\,\mathrm{cm^{-3}}$	$30\,\mathrm{g\,m^{-2}}$
Extratropics	Homogeneous, mean	$107\,\mathrm{cm^{-3}}$	$42\,\mathrm{g\,m^{-2}}$	$73\,\mathrm{cm^{-3}}$	$30\,\mathrm{g\,m^{-2}}$	$125\,\mathrm{cm^{-3}}$	$31\,\mathrm{g\,m^{-2}}$
	median	$50\,\mathrm{cm^{-3}}$	$26\,\mathrm{g\,m^{-2}}$	$45\,\mathrm{cm^{-3}}$	$18\,\mathrm{g\,m^{-2}}$	$89\,\mathrm{cm^{-3}}$	$21\,\mathrm{g\,m^{-2}}$
	Inhomogeneous, mean	$82\,\mathrm{cm^{-3}}$	$48\,\mathrm{g\,m^{-2}}$	$66\,\mathrm{cm^{-3}}$	$42\,\mathrm{g\,m^{-2}}$	$122\,\mathrm{cm^{-3}}$	$38\,\mathrm{g\,m^{-2}}$
	median	$45\,\mathrm{cm^{-3}}$	$36\,\mathrm{g\,m^{-2}}$	$37\,\mathrm{cm^{-3}}$	$24\,\mathrm{g\,m^{-2}}$	$92\,\mathrm{cm^{-3}}$	$26\,\mathrm{g\,m^{-2}}$

Table A1. As Table 1, but separated for ocean, land, Tropics (20° S- 20° N) and Extratropics (40° S - 60° S and 40° N - 60° N).

References

Barahona, D., Sotiropoulou, R., and Nenes, A.: Global distribution of cloud droplet number concentration, autoconversion rate, and aerosol indirect effect under diabatic droplet activation, J. Geophys. Res., 116, D09 203, https://doi.org/10.1029/2010JD015274, 2011.

Barnes, W. L., Pagano, T. S., and Salomonson, V. V.: Prelaunch Characteristics of the Moderate Resolution Imaging Spectroradiometer (MODIS) on EOS-AM1, IEEE Trans. Geosci. Remote Sens., 36, 1088–1100, https://doi.org/10.1109/36.700993, 1998.

Bloom, S., da Silva, A., Dee, D., Bosilovich, M., J-D, Chern, Pawson, S., Schubert, S., and Sienkiewicz, M.: Documentation and Validation of the Goddard Earth Observing System (GEOS) Data Assimilation System-Version 4, Technical Report Series on Global Modeling and Data Assimilation, 26, NASA/TM–2005–104 606, 2005.

Böhm, C., Sourdeval, O., Mülmenstädt, J., Quaas, J., and Crewell, S.: Cloud base height retrieval from multi-angle satellite data, Atmos. Meas. Tech., 12, 1841–1860, https://doi.org/10.5194/amt-12-1841-2019, 2019.

Bony, S., Dufresne, J.-L., Treut, H. L., Morcrette, J.-J., and Senior, C.: On dynamic and thermodynamic components of cloud changes, Clim. Dyn., 22, Issue 2-3, 71–86, 2004.

Boucher, O., Randall, D., Artaxo, P., Bretherton, C., Feingold, G., Forster, P., Kerminen, V.-M., Kondo, Y., Liao, H., Lohmann, U., Rasch, P., Satheesh, S., Sherwood, S., Stevens, B., and Zhang, X.: Clouds and Aerosols, in: Climate Change 2013: The Physical Science Basis. Contribution of Working Group I to the Fifth Assessment Report of the Intergovernmental Panel on Climate Change, edited by Stocker, T., Qin, D., Plattner, G.-K., Tignor, M., Allen, S., Boschung, J., Nauels, A., Xia, Y., Bex, V., and Midgley, P., Cambridge University Press, Cambridge, United Kingdom and New York, NY, USA, https://doi.org/10.1017/CBO9781107415324.016, 2013.

Dhuria, H. L. and Kyle, H. L.: Cloud Types and the Tropical Earth Radiation Budget, J. Climate, 3, 1409–1434, https://doi.org/10.1175/1520-0442(1990)003<1409:CTATTE>2.0.CO;2, 1990.

Grosvenor, D. P., Sourdeval, O., Zuidema, P., Ackerman, A., Alexandrov, M. D., Bennartz, R., Boers, R., Cairns, B., Chiu, C., Christensen, M., Deneke, H., Diamond, M., Feingold, G., Fridlind, A., Hünerbein, A., Knist, C., Kollias, P., Marshak, A., McCoy, D., Merk, D., Painemal, D., Rausch, J., Rosenfeld, D., Russchenberg, H., Seifert, P., Sinclair, K., Stier, P., B. van D., Wendisch, M., Werner, F., Wood, R., Zhang, Z., and Quaas, J.: Remote sensing of cloud droplet number concentration in warm clouds: A review of the current state of knowledge and perspectives, Rev. Geophys., 56, 409–453, https://doi.org/10.1029/2017RG000593, 2018.

Gryspeerdt, E. and Stier, P.: Regime-based analysis of aerosol-cloud interactions, Geophys. Rev. Lett., 39, L21 802, https://doi.org/10.1029/2012GL053221, 2012.

Gryspeerdt, E., Goren, T., Sourdeval, O., Quaas, J., Mülmenstädt, J., S., D., Unglaub, C., Gettelman, A., and Christensen, M.: Constraining the aerosol influence on cloud liquid water path, Atmos. Chem. Phys., 19, 5331–5347, https://doi.org/10.5194/acp-19-5331-2019, 2019.

Hartmann, D. L., Ockert-Bell, M. E., and Michelsen, M. L.: The Effect of Cloud Type on Earth's Energy Balance: Global Analysis, J. Climate, 5, 1281–1304, https://doi.org/10.1175/1520-0442(1992)005<1281:TEOCTO>2.0.CO;2, 1992.

Haynes, J. M., L'Ecuyer, T. S., Stephens, G. L., Miller, S. D., Mitrescu, C., Wood, N. B., and Tanelli, S.: Rainfall retrieval over the ocean with spaceborne W-band radar, J. Geophys. Res., 114, D00A22, https://doi.org/10.1029/2008JD009973, 2009.

Howard, L.: Essay on the modifications of clouds, 1803.

Jakob, C., Tselioudis, G., and Hume, T.: The Radiative, Cloud, and Thermodynamic Properties of the Major Tropical Western Pacific Cloud Regimes, J. Climate, 18, 1203–1215, https://doi.org/10.1175/JCLI3326.1, 2005.

Kato, S., Sun-Mack, S., Miller, W. F., Rose, F. G., Chen, Y., Minnis, P., and Wielicki, B. A.: Relationships among cloud occurrence frequency, overlap, and effective thickness derived from CALIPSO and CloudSat merged cloud vertical profiles, J. Geophys. Res., 115, D00H28, https://doi.org/10.1029/2009JD012277, 2010.

Kato, S., Rose, F. G., Sun-Mack, S., Miller, W. F., Chen, Y., Rutan, D. A., Stephens, G. L., Loeb, N. G., Minnis, P., Wielicki, B. A., Winker, D. M., Charlock, T. P., Jr., P. W. S., Xu, K.-M., and Collins, W. D.: Improvements of top-of-atmosphere and surface irradiance computations with CALIPSO-, CloudSat-, and MODIS-derived cloud and aerosol properties, J. Geophys. Res., 116, D19 209, https://doi.org/10.1029/2011JD016050, 2011.

Kato, S., Miller, W. F., Sun-Mack, S., Rose, F. G., Chen, Y., and Mlynczak, P. E.: Variable Descriptions of the A-Train Integrated CALIPSO, CloudSat, CERES, and MODIS Merged Product (CCCM or C3M), https://eosweb.larc.nasa.gov/project/ceres/readme/c3m_variables_B1_v2.pdf, online; accessed 09-March-2016, 2014.

King, M. D., Menzel, W. P., Kaufman, Y. J., Tanre, D., Bo-Cai, G., Platnick, S., Ackerman, S. A., Remer, L. A., Pincus, R., and Hubanks, P. A.: Cloud and Aerosol Properties, Precipitable Water, and Profiles of Temperature and Water Vapor from MODIS, IEEE Trans. Geosci. Remote Sens., 41, 442–458, https://doi.org/10.1109/TGRS.2002.808226, 2003.

Klein, S. and Hartmann, D.: The seasonal cycle of low stratiform clouds, J. Climate, 6, 1587–1606, https://doi.org/10.1175/1520-0442(1993)006<1587:TSCOLS>2.0.CO;2, 1993.

Medeiros, B. and Stevens, B.: Revealing differences in GCM representations of low clouds, Clim. Dyn., 36, 385–399, https://doi.org/10.1007/s00382-009-0694-5, 2011.

Mülmenstädt, J. and Feingold, G.: The radiative forcing of aerosol-cloud interactions in liquid clouds: Wrestling and embracing uncertainty, Curr. Clim. Change Rep., 4, 23–40, https://doi.org/10.1007/s40641-018-0089-y, 2018.

Mülmenstädt, J., Sourdeval, O., Henderson, D. S., L'Ecuyer, T. S., Unglaub, C., Jungandreas, L., Böhm, C., Russell, L. M., and Quaas, J.: Using CALIOP to estimate cloud-field base height and its uncertainty: The Cloud Base Altitude Spatial Extrapolator (CBASE) algorithm and dataset, Earth Syst. Sci. Data, 10, 2279–2293, https://doi.org/10.5194/essd-10-2279-2018, 2018.

Nam, C. C. and Quaas, J.: Geographically versus dynamically defined boundary layer cloud regimes and their use to evaluate general circulation model cloud parameterizations, Geophys. Res. Lett., 40, 4951–4956, https://doi.org/10.1002/grl.50945, 2013.

Norris, J. R. and Weaver, C. P.: Improved Techniques for Evaluating GCM Cloudiness Applied to the NCAR CCM3, J. Climate, 14, 2540–2550, https://doi.org/10.1175/1520-0442(2001)014<2540:ITFEGC>2.0.CO;2, 2001.

Oreopoulos, L. and Cahalan, R. F.: Cloud Inhomogeneity from MODIS, J. Climate, 18, 5110–5124, https://doi.org/10.1175/JCLI3591.1, 2005.

Painemal, D. and Zuidema, P.: Assessment of MODIS cloud effective radius and optical thickness retrievals over the Southeast Pacific with VOCALS-REx in situ measurements, J. Geophys. Res., 116, D24 206, https://doi.org/10.1029/2011JD016155, 2011.

Park, S. and Shin, J.: Heuristic estimation of low-level cloud fraction over the globe based on a decoupling parameterization, Atmos. Chem. Phys., 19, 5635–5660, https://doi.org/10.5194/acp-19-5635-2019, 2019.

Platnick, S.: Vertical photon transport in cloud remote sensing problems, J. Geophys. Res., 105, 22 919–22 935, https://doi.org/10.1029/2000JD900333, 2002.

Platnick, S., King, M. D., Ackerman, S. A., Menzel, W. P., Baum, B. A., Riedi, J. C., and Frey, R. A.: The MODIS cloud products: algorithms and examples from Terra, IEEE Trans. Geosci. Remote Sens., 41, 459–473, https://doi.org/10.1109/TGRS.2002.808301, 2003.

Quaas, J., Boucher, O., and Lohmann, U.: Constraining the total aerosol indirect effect in the LMDZ and ECHAM4 GCMs using MODIS satellite data, Atmos. Chem. Phys., 6, 947–955, https://doi.org/10.5194/acp-6-947-2006, 2006.

Rienecker, M., Suarez, M., Todling, R., Bacmeister, J., Takacs, L., Liu, H.-C., Gu, W., Sienkiewicz, M., Koster, R., Gelaro, R., Stajner, I., and Nielsen, J.: The GEOS-5 Data Assimilation System-Documentation of Versions 5.0.1, 5.1.0, and 5.2.0, Technical Report Series on Global Modeling and Data Assimilation, 27, NASA/TM–2008–104 606, 2008.

Ringer, M. A. and Allan, R. P.: Evaluating climate model simulations of tropical cloud, Tellus A, 56, 308–327, https://doi.org/10.1111/j.1600-0870.2004.00061.x, 2004.

Rossow, W. B. and Schiffer, R. A.: Advances in Understanding Clouds from ISCCP, Bull. Am. Meteorol. Soc., 80, 2261–2287, https://doi.org/10.1175/1520-0477(1999)080<2261:AIUCFI>2.0.CO;2, 1999.

Shin, J. and Park, S.: The relationship between low-level cloud amount and its proxies over the globe by cloud types, Atmos. Chem. Phys. Discuss., https://doi.org/10.5194/acp-2019-560, 2019.

Stephens, G., Winker, D., Pelon, J., Trepte, C., Vane, D., Yuhas, C., L'Ecuyer, T., and Lebsock, M.: CloudSat and CALIPSO within the A-Train: Ten years of actively observing the Earth system, Bull. Amer. Meteor. Soc., 99, 569–581, https://doi.org/10.1175/BAMS-D-16-0324.1, 2018.

Stephens, G. L., Vane, D. G., Boain, R. J., Mace, G. G., Sassen, K., Wang, Z., Illingworth, A. J., O'Connor, E. J., Rossow, W. B., Durden, S. L., Miller, S. D., Austin, R. T., Benedetti, A., Mitrescu, C., and TEAM, T. C. S.: THE CLOUDSAT MISSION AND THE A-TRAIN: A New Dimension of Space-Based Observations of Clouds and Precipitation, Bull. Am. Meteorol. Soc., 83, 1771–1790, https://doi.org/10.1175/BAMS-83-12-1771, 2002.

Stephens, G. L., Vane, D. G., Tanelli, S., Im, E., Durden, S., Rokey, M., Reinke, D., Partain, P., Mace, G. G., Austin, R., L'Ecuyer, T., Haynes, J., Lebsock, M., Suzuki, K., Waliser, D., Wu, D., Kay, J., Gettelman, A., Wang, Z., and Marchand, R.: CloudSat mission: Performance and early science after the first year of operation, J. Geophys. Res., 113, D00A1810.1029/2008JD009 982, https://doi.org/10.1029/2008JD009982, 2008.

Stevens, B. and Feingold, G.: Untangling aerosol effects on clouds and precipitation in a buffered system, Nature, 461, 607–613, https://doi.org/10.1038/nature08281, 2009.

Su, W., Loeb, N. G., Xu, K., Schuster, G. L., and Eitzen, Z. A.: An estimate of aerosol indirect effect from satellite measurements with concurrent meteorological analysis, J. Geophys. Res., 115, D18 219, https://doi.org/10.1029/2010JD013948, 2010.

Tanelli, S., Durden, S. L., Im, E., Pak, K., Reinke, D., Partain, P., Haynes, J., and Marchand, R.: CloudSat's Cloud Profiling Radar After Two Years in Orbit: Performance, Calibration, and Processing, IEEE Trans. Geosci. Remote Sens., 46, 3560–3573, https://doi.org/10.1109/TGRS.2008.2002030, 2008.

Tselioudis, G., Zhang, Y., and Rossow, W. B.: Cloud and Radiation Variations Associated with Northern Midlatitude Low and High Sea Level Pressure Regimes, J. Climate, 13, 312–327, https://doi.org/10.1175/1520-0442(2000)013<0312:CARVAW>2.0.CO;2, 2000.

Williams, K. D. and Webb, M. J.: A quantitative performance assessment of cloud regimes in climate models, Clim. Dyn., 33, 141–157, https://doi.org/10.1007/s00382-008-0443-1, 2008.

Winker, D. M., Hunt, W. H., and McGill, M. J.: Initial performance assessment of CALIOP, Geophys. Res. Lett., 34, L19 803, https://doi.org/10.1029/2007GL030135, 2007.

Winker, D. M., Vaughan, M. A., Omar, A., Hu, Y., and Powell, K. A.: Overview of the CALIPSO Mission and CALIOP Data Processing Algorithms, J. Atmos. Ocean. Tech., 26, 2310–2323, https://doi.org/10.1175/2009JTECHA1281.1, 2009.

WMO: International cloud atlas, volume I - manual on the observation of clouds and other meteors, http://library.wmo.int/pmb_ged/wmo_407_en-v1.pdf, 1975.

WMO: International cloud atlas, https://cloudatlas.wmo.int, 2017.

Wood, R. and Bretherton, C.: On the relationship between stratiform low cloud cover and lower-tropospheric stability, J. Climate, 19, 6425–6432, https://doi.org/10.1175/JCLI3988.1, 2006.

Wood, R., Leon, D., Lebsock, M., Snider, J., and Clarke, A. D.: Precipitation driving of droplet concentration variability in marine low clouds, J. Geophys. Res., 117, D19 210, https://doi.org/10.1029/2012JD018305, 2012.

Zeng, S., Cornet, C., Parol, F., Riedi, J., , and Thieuleux, F.: A better understanding of cloud optical thickness derived from the passive sensors MODIS/AQUA and POLDER/PARASOL in the A-Train constellation, Atmos. Chem. Phys., 12, 11 245–11 259, https://doi.org/10.5194/acp-12-11245-2012, 2012.